Non-uniform displacement and strain between the soleus and gastrocnemius subtendons of rat Achilles tendon

Finni, T.; Bernabei, M.; Baan, G. C.; Noort, W.; Tijs, C.; Maas, H.

published in
Scandinavian Journal of Medicine and Science in Sports
2018

DOI (link to publisher)
10.1111/sms.13001

document version
Publisher's PDF, also known as Version of record

Accepted: 25 October 2017

DOI: 10.1111/sms.13001

ORIGINAL ARTICLE

WILEY

Non-uniform displacement and strain between the soleus and gastrocnemius subtendons of rat Achilles tendon

T. Finni[1] | **M. Bernabei**[2] | **G. C. Baan**[2] | **W. Noort**[2] | **C. Tijs**[3] | **H. Maas**[2]

[1]Neuromuscular Research Center, Faculty of Sport and Health Sciences, University of Jyväskylä, Jyväskylä, Finland

[2]Department of Human Movement Sciences, Faculty of Behavioural and Movement Sciences, Vrije Universiteit Amsterdam, Amsterdam Movement Sciences, Amsterdam, The Netherlands

[3]Department of Organismic and Evolutionary Biology, Harvard University, Concord Field Station, Bedford, MA, USA

Correspondence
Taija Finni, Neuromuscular Research Center, Faculty of Sport and Health Sciences, University of Jyväskylä, Jyväskylä, Finland.
Email: taija.finni@jyu.fi

Funding information
Netherlands Organization for Scientific Research, Grant/Award Number: 040.11.519; University of Jyväskylä

Achilles tendon (AT) comprises of 3 subtendons arising from the soleus (SOL) and the lateral (LG) and medial (MG) heads of the gastrocnemius muscle. While recent human studies show differential displacement within AT, these displacements have not been attributed to specific subtendons. We tested the hypothesis that the SOL and LG subtendons show differential displacement and strain during various combinations of SOL, LG, and MG excitations. Movement of knots, sutured onto SOL and LG subtendons of 12 Wistar rats, was videotaped, while the muscles were stimulated intramuscularly and ankle torque was assessed. When SOL only was stimulated, the plantar flexion torque was the smallest among the different conditions ($P < .001$). In this condition, from passive to active state, the displacement (0.57 vs 0.47 mm, $P = .002$) and strain (8.4% vs 2.4%, $P < .001$) in the SOL subtendon were greater than in LG subtendon. When LG only was stimulated, a higher ankle torque was measured as compared to SOL stimulation ($P < .001$); the displacement was similar in both subtendons (~0.6 mm), while the strain was greater in LG than in SOL (4.7% vs 1.7%, $P < .001$). When all 3 muscles were stimulated simultaneously, ankle torque was highest and the displacement (0.79 vs 0.74 mm, $P = .002$) and strain (7.7% vs 4.4%, $P = .003$) were greater in SOL than in LG. These data show that the different subtendons of AT can experience relative displacement and differential strains. Together with anatomical dissections, the results revealed that such uniformities may be due to a lower stiffness of SOL subtendon compared to LG.

KEYWORDS
Achilles tendon, anatomy, ankle torque, deformation, 3-dimensional model, triceps surae

1 | INTRODUCTION

The Achilles tendon (AT) bears high loads during everyday movements,[1,2] yet AT is vulnerable to disorders.[3] AT is typically considered as one entity but it consists of 3 distinct subtendons contiguous with soleus (SOL), and lateral (LG) and medial gastrocnemius muscles (MG),[4] which may not always be activated to the same extent.[5] Consequently, one of the etiological factors behind Achilles tendon injuries may be non-uniform stress brought by heterogeneous loading within the tendon.[6,7] While direct measures of stresses within the tendon are invasive, information on non-uniform loading can be achieved based on measures of tendon strain.[8] Strain is typically calculated from tissue displacements assessed by kinematic methods.

Recently, displacements within human tendon have been measured using non-invasive ultrasound-based methods using, for example, commercial speckle tracking[9,10] and radiofrequency data with 2D cross-correlation.[11,12] It was found that the anterior (deep) portion of AT experienced greater displacement during passive ankle movement[9] and eccentric loading of the calf muscles.[11] Furthermore, the anterior portion of AT experienced greater displacement but less elongation than the posterior (superficial) tendon during human walking.[12]

These observations of non-uniform displacements within AT have been attributed to the hierarchical structure of tendon that allows relative sliding of the tendon fascicles[13,14] and to the unique structure of the AT that, in contrast to the most frequent view, contains distinguishable subtendons of SOL, LG, and MG muscles.[15,16] Differences in moment arm lengths, muscle slack lengths, and activation levels between these muscles[12] and orientation of calcaneus[17] may contribute to non-uniform AT behavior.

Previous human studies have also shown relative sliding between SOL and LG muscles, suggesting that AT subtendons are capable—to a certain degree—of moving independently.[18,19] These studies have used selective activation of muscles within the triceps surae group; thus, suggesting that the non-uniform behavior of AT subtendons could be associated with individual muscle activation. However, assessment of the deformation of individual AT subtendons is not yet possible in human studies, due to imaging resolution and selectivity of muscle activation.

Therefore, the purpose of this study was to investigate whether displacement and strain differ between SOL and LG subtendons during various activation conditions in the triceps surae muscles of the rat. It was hypothesized that the subtendons will undergo differential displacement and strain and that these non-uniformities would be most pronounced when SOL or LG muscles are stimulated individually. We also performed an anatomical study to evaluate if AT anatomy in rat is similar to that of human and to reveal potential factors affecting relative displacement and strain.

2 | METHODS

2.1 | Animals

Experiments were performed on 12 adult male Wistar rats (235.5 ± 16.5 g). Surgical and experimental procedures were in strict agreement with the guidelines and regulations concerning animal welfare and experimentation set forth by the Dutch law and were approved by the institutional Committee on Ethics of Animal Experimentation at the Vrije Universiteit Amsterdam. According to standard procedures,[20] the rats were deeply anesthetized by intraperitoneal injection of urethane solution (1.2 mL/100 g body mass, 12.5% urethane solution), as judged by complete absence of withdrawal reflexes. If withdrawal reflexes could be elicited, supplemental doses (0.3-0.5 mL/time) were administered. To prevent hypothermia, animals were placed on an electrical heating pad to keep their core temperature at approximately 37°C. Rats were continuously monitored for body temperature and respiration. After completion of the experiments, the animals were euthanized with an overdose of pentobarbital sodium (Euthasol 20%) injected intracardially, and double-sided pneumothorax. The left (experimental) hindlimb was stored in −40°C for later anatomical study.

2.2 | Surgery and preparation

The left hindlimb was shaved, and the skin covering the lower leg was removed. The femur was exposed, and biceps femoris and gracilis muscles were removed. Anatomical landmarks for axis of rotation of ankle and knee joints were identified and marked with a permanent marker.

The AT was freed from all connective and fat tissues leaving the insertion to calcaneal bone intact. For kinematic analysis, 4 knotted suture markers (Mariderm Schwarz; thread thickness 7/0 USP; Catgut GmbH, Markneukirchen, Germany) were sutured into each of the LG and SOL subtendons (Figure 1). All exposed tissues were regularly irrigated with saline to prevent dehydration.

Following procedures by Tijs et al,[21] the foot was attached to a 6 degrees-of-freedom load cell (Mini40-E, ATI; Apex, NC, USA) and the femur was rigidly secured. During all measurements, the ankle was set at an angle of 120° and the knee at an angle of 90°.

Wire electrodes for intramuscular stimulation were placed near the neuromuscular junctions of SOL, LG, and MG muscles. The location of the neuromuscular junctions was tested by stimulating the muscle superficially with a set current and identifying a location for greatest response. Then, the wires were inserted around this location intramuscularly in bipolar configuration. Stimulation intensity was defined as the intensity resulting in the highest twitch torque.

3 | EXPERIMENTAL PROCEDURES

A trial consisted of 2 conditioning twitches with 1 second in between followed by a 1 second tetanus (stimulation

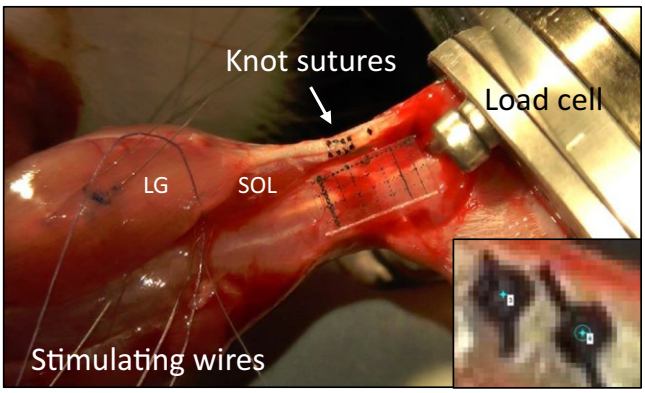

FIGURE 1 Experimental setup showing the left hindlimb attached to a load cell with stimulating wires going into the muscles. Knot sutures in lateral gastrocnemius (top row of knots) and soleus subtendons (bottom row of knots) are seen as black dots. The scale has 1 mm between lines. The inset shows that, during digitizing, the middle of the knot was selected

frequency 100 Hz, pulse width 100 μs, Digitimer DS3, Digitimer Ltd., Hertfordshire, UK). These trials were performed for 5 conditions: stimulation of SOL only (SOLs), LG only (LGs), MG only (MGs), LG and MG simultaneously (LGs + MGs), as well as SOL and LG and MG simultaneously (SOLs + LGs + MGs). Stimulation order was randomized between animals. Two minutes rest was given between trials. To monitor changes in force-producing capacity, control trials with SOLs + LGs + MGs and ankle and knee angles at 90° were performed before and after the experiment. The second control trial was not significantly different from the first but showed individual variation (−0.3%, SD 9.7).

3.1 | Recordings and data analysis

Torque measured by the load cell was sampled at 1000 Hz and stored. Three-dimensional gravity-corrected ankle torques were calculated following previously described procedures.[21] Passive torque was obtained from a 50 ms time window in relaxed condition (after the second twitch). This was subtracted from the torque obtained from a 50 ms window during tetanus to obtain the active torque used in the statistical analysis.

All trials were videotaped at 50 frames/s (HC-V720; Panasonic, Bracknell, UK) for 2-dimensional kinematic analysis of the tendon markers (see Figure 1). A ruler was placed below the tendon from which 5 mm length was digitized and used for calibration. The camera was placed orthogonal to the sagittal plane with focus on the Achilles tendon which yielded an average resolution of 0.023 mm/pixel (range 0.022-0.024).

An image captured in relaxed condition (after the second twitch corresponding to the passive torque) and an image during tetanus (corresponding to the time of active torque) were extracted for further analysis of tendon marker displacements. From these 2 images, the tendon markers were digitized manually by selecting the centroid of the knot (Figure 1), and $[x,y]$ coordinates were extracted. The image analysis was performed using custom-written software in MATLAB (R2014b, MathWorks, Natick, MA, USA).

From the $[x,y]$ coordinates data, displacement (D) of each of the markers (n) from passive to active state (Δx and Δy) was calculated. Then, the average displacement ($\bar{D}$) was calculated as the mean of the 4 SOL and 4 LG marker displacements, respectively.

$$D_n = \sqrt{\Delta x_n^2 + \Delta y_n^2} \quad n = 1,2,3,4$$

$$\bar{D} = \frac{D_1 + D_2 + D_3 + D_4}{4}$$

Strains (ε) based on a linear 3-segment model connecting the 4 markers in SOL and LG subtendons, respectively, were calculated as $\varepsilon = (L\text{-}L_0)/L_0$, where L was the 3-segment length in an active state and L_0 the 3-segment length in the passive state.

LG muscle-tendon unit (MTU) lengths were estimated using an ankle-knee geometric model by Ettema,[22] while SOL MTU lengths were estimated by adjusting the model for ankle joint angle displacement only.[23] The following anatomical parameters, required in the model, were measured from the animals of this study: ankle lever arm length (mean of 6.8 mm used in the model) and tibia length (38.3 mm).

3.2 | Anatomical study

Using a precision caliper, SOL and LG tendon lengths were calculated as the distance between their myotendinous junction and calcaneus while keeping the ankle and knee joint angles at 90°. The distance of the most proximal suture from the myotendinous junction was also measured for complete anatomical information. For all animals, dissection of AT subtendons confirmed that the markers were sutured into either SOL or LG subtendons (Figure 2B).

In 2 animals, an exploratory anatomical study was performed immediately after the stimulation protocol, but before euthanizing the animal. After removing plantaris MTU (Figure 2A), SOL, MG, and LG muscle bellies were dissected from proximal to distal until the tendon. To separate SOL, MG, and LG subtendons, careful blunt dissection along the orientation of tendon fascicles was carried out while minimizing tissue damage. In the most distal part, the separation of SOL, LG, and MG tendons continued by removal of tissue around the calcaneus and the tendon until the insertion sites was fully exposed (Figure 2C).

For 3-dimensional AT reconstruction, the tendon of one animal was prepared in the following manner: AT was first fixed in buffered 4% paraformaldehyde, preserved in buffered 20% sucrose solution, and then taken out of the solution and dried before staining the 3 subtendon surfaces with different colors (Staedtler Permanent Dry Safe, Lumocolor (AP), Germany). Then, AT was embedded in a 4% gelatin solution and frozen before cutting into 1 mm cross-sections. These cross-sections were photographed, and CSAs were measured using ImageJ (imagej.nih.gov) by manually segmenting 5 slices along each of the subtendons. Cross-sectional images were uploaded to Reconstruct (synapseweb.clm.utexas.edu) to create a 3D reconstruction of the AT. Finally, the reconstructed tendon was imported in Anim8or (anim8or.com) and modified to include the insertion onto calcaneus (Figure 3D).

3.3 | Statistics

After confirming normality with Shapiro-Wilk test, by comparing mean and median values and by checking values of

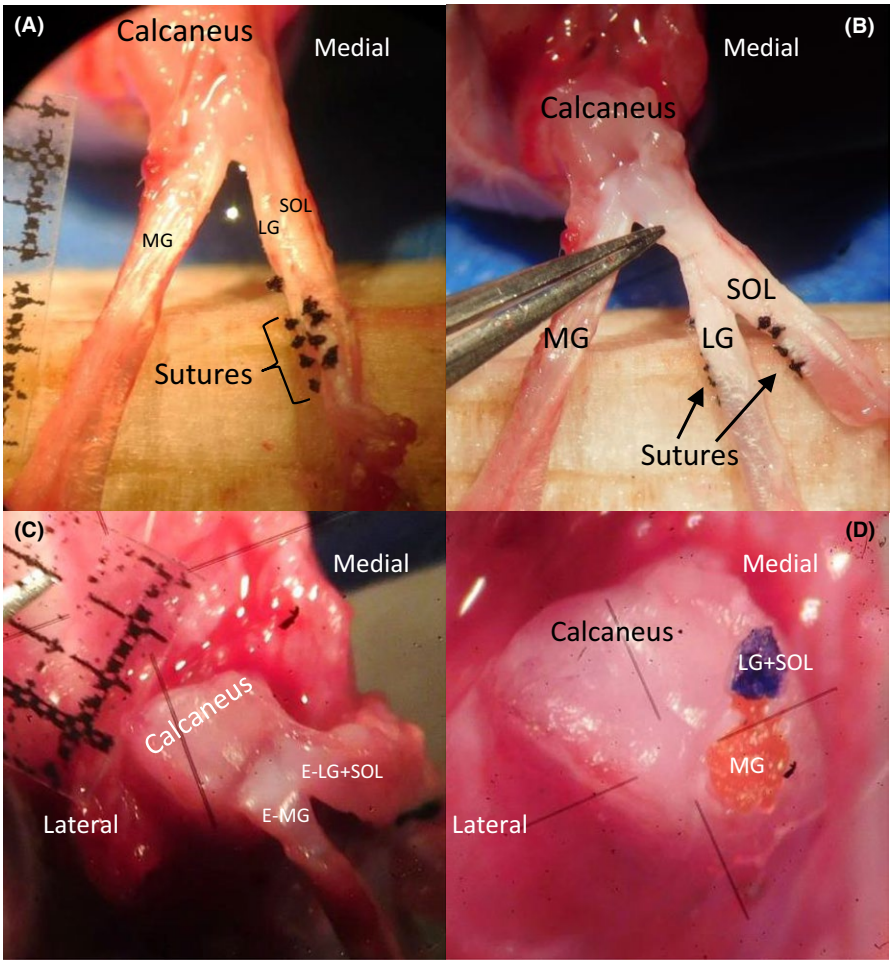

FIGURE 2 A, Achilles tendon has been flipped over calcaneus to reveal dorsal view of the tendon. Medial gastrocnemius tendon (MG) has been separated from lateral gastrocnemius (LG) and soleus (SOL) subtendons. Four sutures along the length of LG and SOL subtendons that were used in the analysis are identified. An additional marker was sutured more distally to the LG, but it was not used in this study. B, Dorsal view of separated LG and SOL subtendons to confirm that the sutures were sown into the correct subtendons. C, A close-up from the tendon insertion to calcaneus via enthesis. E, While MG had a distinguishably its own enthesis, the LG and SOL tendons appeared to share the same enthesis and insertion site. This is also visible in D, where the calcaneus has been fully exposed and tendons detached. The insertion site for MG tendon, marked in red, is larger than the common insertion site for SOL and LG tendons. The scale in A and C has 1 mm between lines

skewness and kurtosis, parametric statistics were used. The effects of stimulation condition on ankle torque were tested using repeated measures ANOVA, while 2-factor ANOVA (stimulation*subtendon) was used to examine differential displacements and strains between the SOL and LG subtendons. Greenhouse-Geisser correction was used when assumption for sphericity was not met and Bonferroni was used as post hoc for pairwise comparisons. Level of significance was set at $P \leq .05$.

4 | RESULTS

4.1 | Tendon anatomy

Mean tendon length was 7.62 mm (SD 0.33) for SOL and 11.22 mm (SD 0.34) for LG. In SOL, the most proximal marker was located 0.26 mm (SD 0.55) distally from the myotendinous junction, and for LG, this distance was 3.89 mm (SD 0.55). Mean resting lengths used in strain calculations (ie, between proximal and distal markers) were 1.56 mm (SD 0.25) for SOL and 1.68 mm (SD 0.35) for LG corresponding to about 20% (SOL) and 15% (LG) of the total tendon lengths. The calculated MTU lengths of SOL and LG were 29.36 mm and 37.46 mm, respectively. LG tendon was 27% and SOL tendon 23% of the estimated MTU length.

The attachment site of the tendons on the calcaneus is shown in Figure 2D. We were not able to identify separate SOL and LG entheses or insertion sites onto the calcaneus (Figure 2C). The attachment area of SOL + LG was slightly smaller than that for MG, the latter being located laterally to the attachment site of SOL + LG. The model of AT illustrates that the MG travels from medial to postero-lateral side, while LG travels medially when traveling distally (Figure 3). Mean cross-sectional area of the subtendon was 0.14 mm^2 for SOL, 0.34 mm^2 for LG, and 0.48 mm^2 for MG.

4.2 | Ankle joint torque

Stimulation condition had a main effect on ankle torque ($P < .001$) with all other conditions differing from each other except LGs and MGs. Ankle torque was smallest when SOL was stimulated and highest when all 3 muscles were stimulated (Figure 4A). LG ankle torque (16.9 ± 5.6 mNm) was over 4 times higher and MG torque (12.8 ± 2.9 mNm) over 3 times higher than SOL torque (3.9 ± 2.4 mNm).

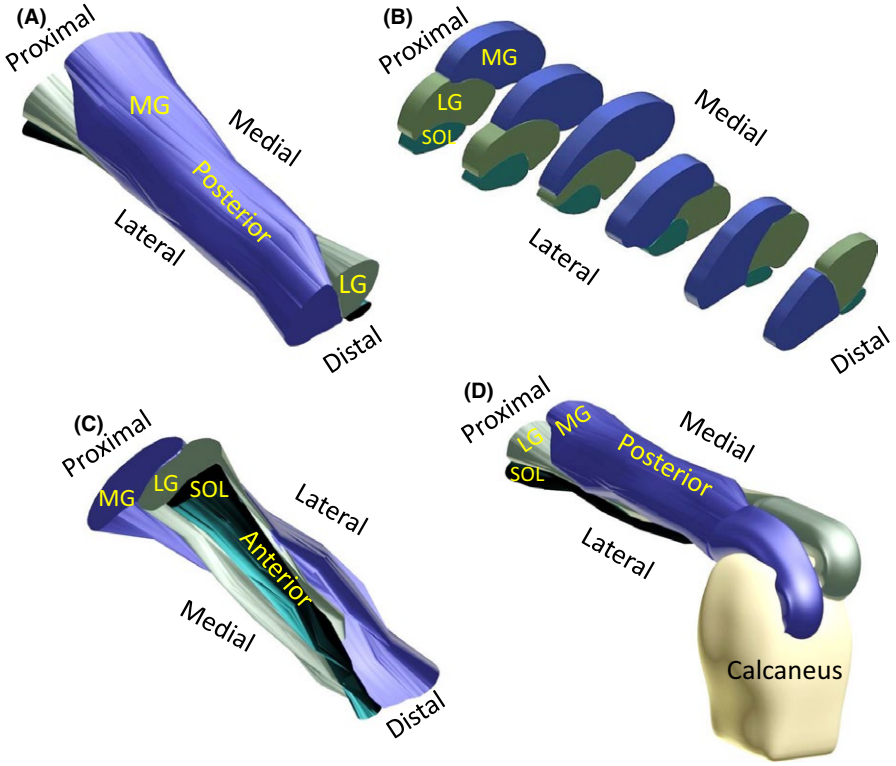

FIGURE 3 Three-dimensional reconstruction of the rat Achilles tendon (AT). Similarly to human AT, the model illustrates medio-lateral twist of the rat medial gastrocnemius (MG) subtendon (A, B, C). Subtendon of lateral gastrocnemius (LG) travels medially emerging underneath the MG to its lateral attachment site in the calcaneus (D). Contrary to humans, rat soleus (SOL) muscle and its respective subtendon comprise a small cross-sectional area relative to MG and LG (B)

4.3 | Displacement of subtendons

Both subtendons showed displacements even if their respective muscle was not stimulated. Displacements of SOL and LG subtendons differed for some, but not all, stimulation conditions (Figure 4B). Main effects of stimulation condition ($P = .001$) and subtendon ($P = .003$) on tendon displacements were found as well as a significant stimulation*subtendon interaction effect ($P = .002$). Post hoc pairwise comparisons revealed differences between subtendons (Figure 4B) and between the following stimulation conditions: LGs and SOLs + LGs + MGs (on average 24% greater displacement with SOLs + LGs + MGs, $P = .016$), MGs and LGs + MGs (43%, $P = .003$), and MGs and SOLs + LGs + MGs (52%, $P = .002$).

4.4 | Subtendon strain

There was a main effect of stimulation ($P < .001$) and subtendon ($P = .017$) on SOL and LG subtendon strain with significant interaction ($P < .001$). Post hoc pairwise comparisons showed that SOL and LG subtendon strains were different in each stimulation condition (Figure 4C). Overall, subtendon strains in SOLs condition differed from LGs ($P = .022$), MGs ($P < .001$), and LGs + MGs conditions ($P < .001$). Strain also differed between LGs and MGs ($P < .001$), LGs and LGs + MGs ($P = .021$), MGs and LGs + MGs ($P < .000$), MGs and SOLs + LGs + MGs ($P < .001$), and LGs + MGs and SOLs + LGs + MGs ($P = .003$) conditions. Note that in both conditions when SOL was stimulated, SOL tendon was stretched to a greater extent than LG tendon.

5 | DISCUSSION

Typically, the AT is considered as one entity but it consists of 3 distinct subtendons contiguous with SOL, LG, and MG muscles. This study investigated to what extent SOL and LG subtendons displacement and strain differ during various activation conditions of the triceps surae muscles. We found differential displacements for the SOL and LG subtendons in some, but not all, conditions and different strains when the triceps surae muscles were activated individually or simultaneously. This is in agreement with human imaging studies reporting non-uniform displacements within AT (eg,[9,11,12]) and confirms the earlier notion that a single measure of strain may not provide an accurate representation of the AT behavior as a whole.[24] In spite of the observed non-uniform strain, our findings suggest that the distinct subtendons are not completely independent because activation of any combination of the muscles produced displacements of similar order of magnitude in both SOL and LG subtendons (Figure 4B).

We hypothesized that the differences in SOL and LG subtendon behavior would be the greatest when their respective muscles were stimulated individually. This was true when only SOL was stimulated; both the displacement and strain in the SOL subtendon were significantly higher than in the LG subtendon. However, when only LG was stimulated the

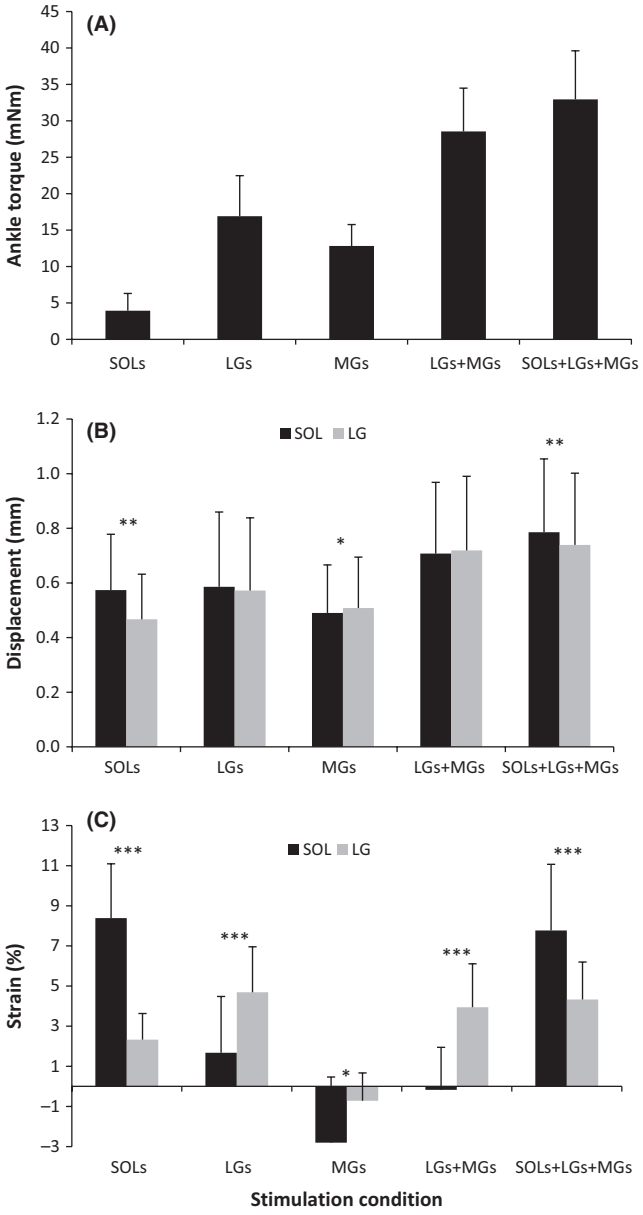

FIGURE 4 Mean (SD) of ankle joint torque (A), subtendon displacement (B), and strain (C) in the 5 different stimulation conditions; only soleus: SOLs, only lateral gastrocnemius: LGs, only medial gastrocnemius: MG, LG and MG simultaneously: LGs + MGs, and all 3 muscles together: SOLs + LGs + MGs. Ankle torque differed significantly ($P \leq .001$) between all conditions except between LGs and MGs. Differences between subtendons; *$P < .05$, **$P < .01$, ***$P < .001$

displacement was similar in both subtendons while the strain was greater in LG. This result may indicate that activation of a single muscle results in a pulling force on the neighboring subtendon without stretching it much. The observed asymmetries in deformations of SOL and LG subtendons may come from the differences in anatomy and properties of the MTU and/or asymmetries in the connective tissue linkages between these muscles.

As shown in Figure 4, when SOL was activated individually it produced the smallest ankle torque but strained the SOL subtendon by ~8% while activation of SOL together with LG and MG produced much greater ankle torque but a similar strain in SOL subtendon. The LG subtendon, on the other hand, strained ~4% in the conditions when its muscle was stimulated individually or simultaneously with other muscles. When all muscles were stimulated simultaneously, SOL subtendon strain was nearly twofold compared to LG strain. The results show convincingly that tendons lengthen and store elastic energy even in small animals.

Using the torque and strain values of Figure 4, we may conclude that the SOL subtendon has a lower stiffness than that of LG. However, considering that the LG tendon had a larger CSA, their Young's modulus can still be quite similar. Previously, considerable variation in tendon material properties has been reported in various tendons of lower limb of turkeys but with rather similar maximum strain of ~10%.[25] Considering that in the current, supposedly submaximal activation condition, the SOL subtendon strained up to ~8%, the observation raises question about the susceptibility of SOL subtendon to injuries in tasks requiring maximal effort.

Based on the previously reported non-uniform AT displacements from human experiments, the following question has been asked: why would the free AT, representing the tendon length from the distal end of SOL muscle belly to the calcaneus (ie, SOL subtendon), show a greater elongation than the longer tendon of the gastrocnemius muscle?[26] The present results suggest that the tendon properties may vary within the AT. While anatomical and functional differences between human and rat triceps surae MTU must be considered, in both species, the SOL subtendon is located anteriorly (Figure 3).[15-17] In agreement with our results in the rat AT, the anterior part of the human AT has been shown to elongate and strain more than posterior tendon where the gastrocnemius subtendons are located.[9,11]

While these human studies were not able to specify if the anterior part could be attributed to SOL subtendon, several ultrasound studies have accomplished to separate SOL and MG tendons by assessing displacement of their respective muscle-tendon junctions.[27-29] During isometric contraction, these studies showed strains of 5.2% in SOL vs 2.6% in MG,[27] 6.6% in SOL vs 2.6% in MG,[28] and 3.8% in SOL vs 2.7% in MG,[29] which are slightly lower than those in the present rat study (7.8% in SOL vs 4.3% in LG in the condition where all 3 muscles were stimulated). Despite different species, activation type (voluntary vs intramuscular stimulation), and level of contraction, data from the present and previous studies lead to the conclusion that SOL strains more than LG during isometric contraction.

However, a different behavior was observed in the intact compartment and with a physiological pattern of activation. During the stance phase of walking in rats, length change up

to about 3.1 mm in LG and 0.9 mm in SOL distal tendons have been reported.[23] This corroborates with finding of Franz et al[12] that the posterior AT had greater elongation than anterior AT during walking. This discrepancy between isometric and dynamic conditions might be explained by the fact that during walking also knee joint angle changes and the deformations of different subtendons may thus differ from purely isometric conditions.

Comparing strain between the subtendons eliminates the differences in absolute length from consideration but observations of their relative movements may also be important. Large relative movements in adjacent tendon fascicles or subtendons may be expected to damage the intrafascicular matrix and smaller relative movements can also lead to injury after repetitive loading, for example Ref.[30] In the present study, the displacement in SOL was slightly but significantly greater than in LG in 3 of 5 stimulation conditions (Figure 4B). The magnitude of relative movement was in the order of tenth of a millimeter, and it may be considered that the displacements were similar between the subtendons. These similarities in displacements may indicate that at least part of the AT acts as a common spring for the muscle compartments of the triceps surae.[31] Similar displacements, even if only one muscle was stimulated, could also be caused by connective tissue linkages between the muscle bellies or subtendons. Future studies should explore what is the degree of dependency between the subtendons and how their behavior is related to subtendon properties, relative muscle length, and activation level of the triceps surae muscles.

5.1 | Anatomy

Similar to the human AT, the reconstructed model of the rat AT (Figure 3) shows rotation of MG subtendon from medial origin to lateral insertion site.[16] In rats, this anatomical organization has been suggested to cause an eversion moment at the ankle joint.[21] In humans, however, MG has been reported to contribute either to eversion or inversion depending on the frontal plane angle of the foot.[32] In the present study, LG attachment was located to lateral aspect of calcaneus together with SOL. In humans, considerable variations in the attachment patterns of the 3 tendons have been found.[33] Unlike in human AT, the insertion site of rat MG to calcaneus was larger than that of SOL and LG, and these 2 tendons seemed to share the same enthesis. In rats, the joint enthesis of SOL and LG may be a necessity due to the small cross-sectional area of the SOL tendon, the arrangement providing reinforcement to the insertion site.

The hierarchical structure of tendon with interactions between collagen fibers and the matrix they are embedded in has been a challenge for modeling studies. Because AT injuries are rather common, modeling attempts are important for this specific tendon as well. It has already been shown that subject-specific geometry of total AT may explain rupture location,[34] and the next step would be to incorporate the subtendon organization and properties of interfascicular matrix to such models.

5.2 | Limitations

It is important to note that we did not fully excite these muscles, and, thus, ankle torque does not reflect the maximal force capacity of these muscles. While we placed the electrodes as close to the point that yielded largest twitch when stimulated from the surface of the muscle and used the intensity that elicited maximal twitch, not all the motor units could be recruited. It has been reported that the LGs + MGs peak active ankle moment may be only about 20% when activated intramuscularly as compared to nerve stimulation.[21] However, at least for SOL muscle, we may have been closer to 50% of maximal isometric torque as the torque was about 4 mNm in the present study as compared to 8 mNm with supramaximal nerve stimulation.[21] Overall, the torques exerted by the various muscles were in line with what is expected based on muscle sizes and assuming similar moment arms around the ankle for all muscles.[35]

The kinematic measures were carried out in one plane only. The 2-dimensional approach causes some uncertainties in the reported displacement and strain values due to out-of-plane movement and possible rotation of the tendon. Estimating a 10° difference between the imaging and movement planes would have caused about 1.5% error in the displacements reported in this study. When discussing the reported displacements, it needs to be acknowledged that they were tracked from a part of the tendon, not from its entire length. In SOL muscle, the tracking was performed as proximally as possible whereas the adjacent markers in MG lay in the mid-tendon. Potential longitudinal differences in tendon properties could therefore be one reason for the observed differential behavior. While MG tendon deformation could not be measured in the present study due to limitations of the 2-dimensional kinematic method used, the effects of MG stimulation on SOL and LG subtendons were somewhat unexpected. The negative strains observed upon MG activation suggest that the most distal parts of LG and SOL subtendons were pulled proximally relative to the most proximal part, or that this result is due to errors from inability of the 2-dimensional analysis to quantify tendon rotation.

6 | PERSPECTIVE

Achilles tendon comprises of 3 distinct subtendons that can behave differently. We showed that, during isometric contractions, the SOL subtendon undergoes substantially greater strain than LG subtendon when their respective muscles are

stimulated independently or simultaneously. We conclude that one cause for the non-uniform behavior within the rat AT may be different stiffness of the subtendons, SOL being more compliant than LG. The difference in strain between the subtendons necessitates a degree of non-uniform displacement between the subtendons. While the elastic interfascicular matrix allows relative sliding of the tendon fascicles, it can also bear considerable loads. With a stiffness about half of that of tendon fascicles,[30,36] the matrix can act to distribute forces within the tendon or serve as an alternative pathway for force transmission upon damage to tendon fascicles. Consequently, tendon organization may provide an inbuilt protective mechanism against tendon injuries by shielding tendon from uneven stresses caused by differences in SOL, LG, and MG activation levels in combination with differential MTU length changes between the triceps surae muscles during normal physical activities. Future studies are needed to reveal which structures, such as the tendon matrix properties[36] or connective tissue links between the muscle bellies,[37] bring about the mechanical dependency of the subtendons.

ACKNOWLEDGEMENTS

This research was carried out during a visit from TF to HM, which was supported by a visitor's travel grant from the Netherlands Organization for Scientific Research [040.11.519] and University of Jyväskylä.

ORCID

T. Finni http://orcid.org/0000-0002-7697-2813

REFERENCES

1. Komi PV. Relevance of in vivo force measurements to human biomechanics. *J Biomech*. 1990;23:23-34.
2. Finni T, Komi PV, Lukkariniemi J. Achilles tendon loading during walking: application of the novel optic fiber technique. *Eur J Appl Physiol*. 1998;77:289-291.
3. Lantto I, Heikkinen J, Flinkkilä T, Ohtonen P, Leppilahti J. Epidemiology of Achilles tendon ruptures: increasing incidence over a 33-year period. *Scand J Med Sci Sports*. 2015;25:133-138.
4. Handsfield GG, Slane LC, Screen HRC. Nomenclature of the tendon hierarchy: an overview of inconsistent terminology and a proposed size-based naming scheme with terminology for multi-muscle tendons. *J Biomech*. 2016;49:3122-3124.
5. Moritani T, Oddsson L, Thorstensson A. Phase-dependent preferential activation of the soleus and gastrocnemius muscles during hopping in humans. *J Electromyogr Kinesiol*. 1991;1:34-40.
6. Arndt AN, Komi PV, Brüggemann G-P, Lukkariniemi J. Individual muscle contributions to the in vivo Achilles tendon force. *Clin Biomech*. 1998;13:532-541.
7. Bojsen-Møller J, Magnusson SP. Heterogeneous loading of the human Achilles tendon in vivo. *Exerc Sport Sci Rev*. 2015;43:190-197.
8. Almekinders LC, Vellema JH, Weinhold PS. Strain patterns in the patellar tendon and the implications for patellar tendinopathy. *Knee Surg Sports Traumatol Arthrosc*. 2002;10:2-5.
9. Arndt A, Bengtsson A-S, Peolsson M, Thorstensson A, Movin T. Non-uniform displacement within the Achilles tendon during passive ankle joint motion. *Knee Surg Sports Traumatol Arthrosc*. 2012;20:1868-1874.
10. Fröberg Å, Cissé AS, Larsson M, et al. Altered patterns of displacement within the Achilles tendon following surgical repair. *Knee Surg Sports Traumatol Arthrosc*. 2017;25:1857-1865.
11. Slane LC, Thelen DG. Non-uniform displacements within the Achilles tendon observed during passive and eccentric loading. *J Biomech*. 2014;47:2831-2835.
12. Franz JR, Thelen DG. Depth-dependent variations in Achilles tendon deformations with age are associated with reduced plantarflexor performance during walking. *J Appl Physiol*. 2015;119:242-249.
13. Benjamin M, Kaiser E, Milz S. Structure-function relationships in tendons: a review. *J Anat*. 2008;212:211-228.
14. Haraldsson BT, Aagaard P, Qvortrup K, et al. Lateral force transmission between human tendon fascicles. *Matrix Biol*. 2008;27:86-95.
15. Szaro P, Witkowski G, Smigielski R, Krajewski P, Ciszek B. Fascicles of the adult human Achilles tendon—an anatomical study. *Ann Anat*. 2009;191:586-593.
16. Edama M, Kubo M, Onishi H, et al. The twisted structure of the human Achilles tendon. *Scand J Med Sci Sports*. 2015;25:497-503.
17. Lersch C, Grötsch A, Segesser B, Koebke J, Brüggemann GP, Potthast W. Influence of calcaneus angle and muscle forces on strain distribution in the human Achilles tendon. *Clin Biomech*. 2012;27:955-961.
18. Bojsen-Møller J, Schwartz S, Kalliokoski KK, Finni T, Magnusson SP. Intermuscular force transmission between human plantarflexor muscles in vivo. *J Appl Physiol*. 2010;109:1608-1618.
19. Finni T, Cronin NJ, Mayfield D, Lichtwark GA, Cresswell AG. Effects of muscle activation on shear between human soleus and gastrocnemius muscles. *Scand J Med Sci Sports*. 2015;27:26-34.
20. Maas H, Baan GC, Huijing PA. Intermuscular interaction via myofascial force transmission: effects of tibialis anterior and extensor hallucis longus length on force transmission from rat extensor digitorum longus muscle. *J Biomech*. 2001;34:927-940.
21. Tijs C, van Dieën JH, Baan GC, Maas H. Three-dimensional ankle moments and nonlinear summation of rat triceps surae muscles. *PLoS One*. 2014;9:e111595.
22. Ettema GJ. Gastrocnemius muscle length in relation to knee and ankle joint angles: verification of a geometric model and some applications. *Anat Rec*. 1997;247:1-8.
23. Bernabei M, van Dieën JH, Maas H. Longitudinal and transversal displacements between triceps surae muscles during locomotion of the rat. *J Exp Biol*. 2017;220:537-550.
24. Finni T, Hodgson JA, Lai A, Edgerton VR, Sinha S. Nonuniform strain of human soleus aponeurosis-tendon complex during submaximal voluntary contractions in vivo. *J Appl Physiol*. 2003;95:829-837.
25. Matson A, Konow N, Miller S, Konow PP, Roberts TJ. Tendon material properties vary and are interdependent among turkey hindlimb muscles. *J Exp Biol*. 2012;215:3552-3558.
26. Finni T, Lichtwark GA. Rise of the tendon research. *Scand J Med Sci Sports*. 2016;26:992-994.

27. Farris DJ, Trewartha G, McGuigan MP, Lichtwark GA. Differential strain patterns of the human Achilles tendon determined in vivo with freehand three-dimensional ultrasound imaging. *J Exp Biol*. 2013;216:594-600.
28. Obst SJ, Newsham-West R, Barrett RS. Changes in Achilles tendon mechanical properties following eccentric heel drop exercise are specific to the free tendon. *Scand J Med Sci Sports*. 2016;26:421-431.
29. Lichtwark GA, Cresswell AG, Newsham-West RJ. Effects of running on human Achilles tendon length-tension properties in the free and gastrocnemius components. *J Exp Biol*. 2013;216:4388-4394.
30. Thorpe CT, Riley GP, Birch HL, Clegg PD, Screen HR. Fascicles and the interfascicular matrix show adaptation for fatigue resistance in energy storing tendons. *Acta Biomater*. 2016;42:308-315.
31. Sandercock TG, Maas H. Force summation between muscles: are muscles independent actuators? *Med Sci Sports Exerc*. 2009;41:184-190.
32. Lee SS, Piazza SJ. Inversion-eversion moment arms of gastrocnemius and tibialis anterior measured in vivo. *J Biomech*. 2008;41:3366-3370.
33. Edama M, Kubo M, Onishi H, et al. Structure of the Achilles tendon at the insertion on the calcaneal tuberosity. *J Anat*. 2016;229:610-614.
34. Shim VB, Fernandez JW, Gamage PB, et al. Subject-specific finite element analysis to characterize the influence of geometry and material properties in Achilles tendon rupture. *J Biomech*. 2014;47:3598-3604.
35. Woittiez RD, Baan GC, Huijing PA, Rozendal RH. Functional characteristics of the calf muscles of the rat. *J Morphol*. 1985;184:375-387.
36. Thorpe CT, Godinho MSC, Riley GP, Birch HL, Clegg PD, Screen HRC. The interfascicular matrix enables fascicle sliding and recovery in tendon, and behaves more elastically in energy storing tendons. *J Mech Behav Biomed Mater*. 2015;52:85-94.
37. Maas H, Sandercock TG. Force transmission between synergistic skeletal muscles through connective tissue linkages. *J Biomed Biotechnol*. 2010;2010:575672.

How to cite this article: Finni T, Bernabei M, Baan GC, Noort W, Tijs C, Maas H. Non-uniform displacement and strain between the soleus and gastrocnemius subtendons of rat Achilles tendon. *Scand J Med Sci Sports*. 2018;28:1009–1017. https://doi.org/10.1111/sms.13001